Analytical Methods

www.rsc.org/methods

Volume 5 | Number 7 | 7 April 2013 | Pages 1631–1888

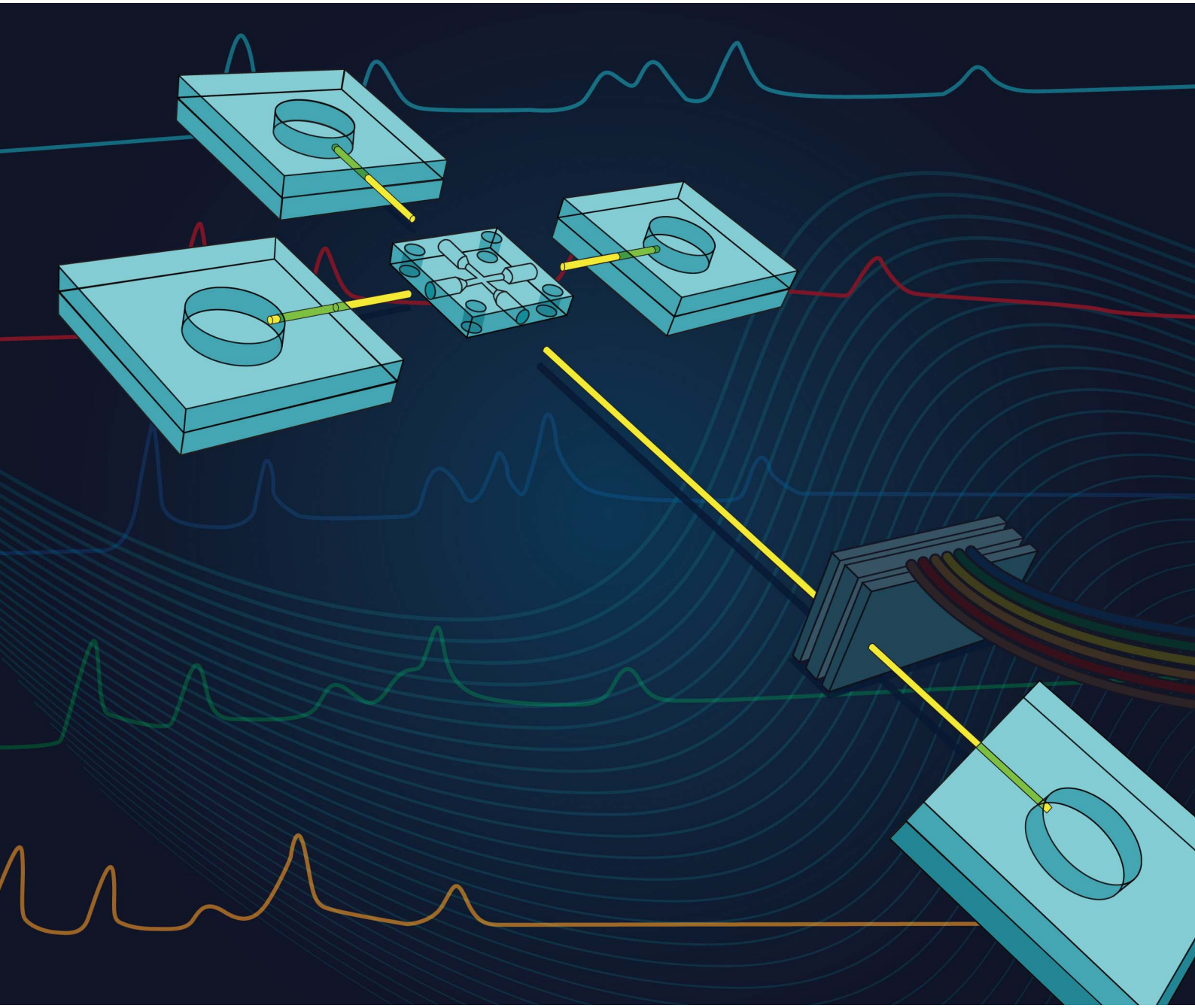

ISSN 1759-9660

RSC Publishing

PAPER

Garcia *et al.*

Microfab-less microfluidic capillary electrophoresis devices

1759-9660(2013)5:7;1-Z

Analytical Methods

RSC Publishing

PAPER

View Article Online
View Journal | View Issue

Microfab-less microfluidic capillary electrophoresis devices†

Cite this: *Anal. Methods*, 2013, **5**, 1652

Thiago P. Segato,[a] Samir A. Bhakta,[b] Matthew T. Gordon,[b] Emanuel Carrilho,[a] Peter A. Willis,[c] Hong Jiao[d] and Carlos D. Garcia*[b]

Compared to conventional benchtop instruments, microfluidic devices possess advantageous characteristics including great portability potential, reduced analysis time (minutes), and relatively inexpensive production, putting them on the forefront of modern analytical chemistry. Fabrication of these devices, however, often involves polymeric materials with less-than-ideal surface properties, specific instrumentation, and cumbersome fabrication procedures. In order to overcome such drawbacks, a new hybrid platform is proposed. The platform is centered on the use of 5 interconnecting microfluidic components that serve as either the injector or reservoirs. These plastic units are interconnected using standard capillary tubing, enabling in-channel detection by a wide variety of standard techniques, including capacitively coupled contactless conductivity detection (C^4D). Due to the minimum impact on the separation efficiency, the plastic microfluidic components used for the experiments discussed herein were fabricated using an inexpensive engraving tool and standard Plexiglas. The presented approach (named 5^2-platform) offers a previously unseen versatility, enabling the assembly of the platform within minutes using capillary tubing that differs in length, diameter, or material. The advantages of the proposed design are demonstrated by performing the analysis of inorganic cations by capillary electrophoresis on soil samples from the Atacama Desert.

Received 13th November 2012
Accepted 27th January 2013

DOI: 10.1039/c3ay26392d

www.rsc.org/methods

1 Introduction

Microchip – capillary electrophoresis (μchip-CE) devices are part of a trend combining portability, miniaturization, and low cost with high analytical performance. Considering a variety of potentially customizable parameters including separation media, material substrate, fabrication method, and detection scheme, these small devices are capable of handling chemical analyses across a broad spectrum of disciplines.[1–4] Additionally, μchip-CE offers a number of advantages over traditional benchtop instrumentation such as lower volumes of sample and reagents, shorter analysis times, and the capacity to operate in a fully automated fashion.[5,6]

Microchips were initially developed from glass substrates through photolithography and a variety of etching techniques.[7–9] Although glass has almost ideal optical properties and well-known surface chemistry, the fabrication protocols are expensive, lengthy, and typically yield rather fragile chips that can be ruined even by small particles clogging a channel. Among other materials (most often polymers) that have been extensively utilized for fabrication,[10,11] it is worth mentioning poly(methyl methacrylate) (PMMA),[12] polycarbonate,[13] and poly(dimethylsiloxane).[14,15] One of the main advantages of these polymeric materials is that they allow fast and cost-efficient fabrication of devices by a variety of techniques including laser ablation,[16] hot embossing,[17,18] and microwave bonding.[19] Additionally, a variety of procedures are currently available to modify the surface of these materials.[20–25] More recently, polyester-toner[26] and paper-based microfluidic devices[27–29] have emerged as promising platforms for microfluidic applications. In both cases, the devices can be produced by a direct-printing process and represent one of the simplest available technologies for microchip production (less than $0.10 per device).

Although all of these methods have yielded examples of functioning microfluidic devices, it is clear that there is a trade-off between the fabrication procedure, the material, and the microdevice performance. In other words, high-performing devices are still expensive and low-cost devices only offer limited analytical performance. There are also a variety of standard chips commercially available, but these items are expensive and inherently non-reconfigurable. For analysis in remote areas or locations where microfabrication facilities are unavailable, on-site reconfiguration could be required, limiting the versatility of the standard approach utilizing glass microchips.

[a]*Instituto de Quimica de São Carlos, Universidade de São Paulo, São Carlos, SP, Brazil*
[b]*Department of Chemistry, UT San Antonio, One UTSA Circle, San Antonio, TX 78249, USA. E-mail: carlos.garcia@utsa.edu; Fax: +1 210 458-7428; Tel: +1 210 458-5774*
[c]*NASA/Jet Propulsion Laboratory, Pasadena, CA, USA*
[d]*HJ Science & Technology, Santa Clara, CA, USA*

† Electronic supplementary information (ESI) available. See DOI: 10.1039/c3ay26392d

Aiming to overcome such drawbacks, a series of modular (plug-n-play) microfluidic systems have been proposed.[30–33] These devices add tremendous flexibility to the design but are typically limited to hydrodynamic pumping and most often require microfabrication facilities. Alternatively, this manuscript describes a microchip-inspired platform based on 5 plastic microfluidic components that serve as the injector (1 cm × 1 cm × 0.4 cm) or reservoirs (1.9 cm × 1.9 cm × 0.6 cm). These components are interconnected using standard capillary tubing, enabling in-channel detection by a wide variety of standard techniques, including C^4D (demonstrated in this manuscript), as well as electrochemical or optical methods. The resulting devices are suitable for capillary electrophoresis, avoid the use of specific machinery or microfabrication facilities, are inexpensive (less than $70 per re-usable setup), and are assembled (or reconfigured) in just a few minutes. Such features make this platform a worthy candidate to have a high impact in society because it could be replicable for didactic purposes, and it could make the field of microfluidics accessible to low-resource communities. The capabilities of the resulting device were demonstrated by performing an analysis of representative inorganic cations in soil samples from the Atacama Desert.

2 Materials and methods

Reagents and solutions

All chemicals were analytical reagent grade and used as received. The analytes (KCl, NaCl, LiCl, $CaCl_2$, $MgCl_2$) and NaOH were purchased from Sigma-Aldrich (Saint Louis, MO); $(NH_4)_2SO_4$ was purchased from MCB (Darmstadt, Germany). Aqueous solutions were prepared using 18 MΩ-cm water (NANOpure Diamond, Barnstead; Dubuque, Iowa) and were filtered using a hollow fiber filter (0.2 μm, Barnstead). The pH of the solutions was adjusted when necessary, using either 1 mol L^{-1} NaOH or 1 mol L^{-1} HCl (Fisher Scientific; Fair Lawn, NJ) and measured using a glass electrode and a digital pH meter (Orion 420A+, Thermo; Waltham, MA). The background electrolyte (BGE) used for all the experiments was prepared from a stock solution of 100 mmol L^{-1} 2-(*N*-morpholino)ethanesulfonic acid (MES) and 100 mmol L^{-1} L-histidine (HIS). Stock solutions of each analyte (10 mmol L^{-1} each) were prepared daily in DI water and then diluted in the running buffer prior to analysis.

Electrophoretic system

The system was assembled by connecting 4 PMMA reservoirs to a central interconnect (Ultem® Cross C360-204, Labsmith; Livermore, CA) *via* standard silica capillary tubing (50 μm ID, 360 μm OD; Polymicro Tech; Phoenix, AZ). The solution reservoirs were fabricated by cutting squares of 1.9 cm × 1.9 cm from standard layers of PMMA (1/16″ thick) using a computer-controlled engraver (Gravograph IS400, Gravotech; Duluth, GA).‡ These squares were denoted as "top" and "bottom". While the "bottom" layer consists of a flat piece of PMMA, the "top" unit has a hole drilled into the PMMA that serves as the well for sample/buffer/waste and also contains a fine channel to connect the capillary tubing. In order to avoid leaks, the capillary tubing was first glued to the "top" piece with "PMMA glue" (PMMA dissolved in chloroform) and then thermally sealed to the "bottom" piece at 120 ± 3 °C for 15 min. The reservoirs fabricated in this manner were connected to one another *via* an interconnect (1 cm × 1 cm × 0.4 cm), forming the microchip-inspired platform schematically shown in Fig. 1. Connection between the central square and the capillaries was performed using four PEEK fittings (360 μm, Labsmith; Livermore, CA). The system was assembled under water to prevent formation of air bubbles during the application of the electrophoretic potential. In order to calculate the volume of the interconnecting square, one of the pieces was sanded to half height and visualized using a 3D laser microscope (Olympus LEXT). The picture inset in Fig. 1 shows that the connector comprises inner channels of approximately 250 μm, which are larger than standard injectors specifically designed for microchip applications. The dead volume of the interconnect (according to the manufacturer) is 38 nL.

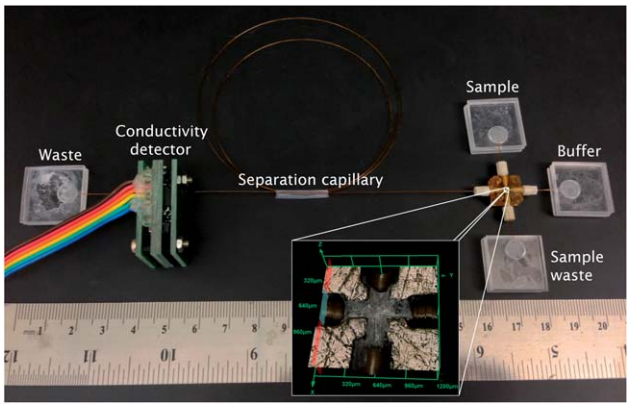

Fig. 1 Picture of the 5^2 platform assembled from the 5 squares and capillaries. Inset showing a microphotograph of the central interconnect (1.28 mm × 1.28 mm).

The system was washed daily with 0.1 mol L^{-1} NaOH, ultrapure water, and running buffer for 30 min each. This procedure was adopted to activate the fused silica surface and promote higher and stable electro-osmotic flow (EOF). Between each injection, the capillary was rinsed with running buffer for 20 min. The sample injection was performed by applying vacuum of ~70 kPa on the sample waste reservoir for a selected period of time. After the application of the vacuum, the reservoir was replenished with running buffer. To perform the electrophoretic separation, a selected potential was applied to the buffer reservoir, with respect to the ground electrode, which was placed in the buffer waste reservoir. For all experiments involving electrophoresis, a high-voltage rack (HV-RACK-4-250, Ultravolt; Ronkonkoma, NY) was used. The openC^4D (https://sites.google.com/site/openc4d/) detector was obtained from the University of Sao Paulo in Brazil and used in the format described by Francisco and do Lago.[34] The electronic circuitry of the C^4D includes a signal generator, a detection cell, a transimpedance amplifier, a rectifier, a low-pass filter, and an

‡ Alternatively, these pieces can be fabricated with a standard saw and drill set.

analog-to-digital converter. The arrangement includes two 2 mm coiled copper electrodes separated by a gap of 0.51 mm. Data acquisition was obtained using the *Swing CE* software supplied with the openC^{4}D and the experimental conditions for the detector include using a sine wave with a frequency of 1.1 MHz with an amplitude of 4 V (peak-to-peak).

Soil samples

Soil samples were collected from the Atacama Desert (northern Chile) in June 2005. Due to the extreme aridity of this region (experiencing less than a centimeter of precipitation per decade) and the chemical/mineralogical composition of the surface materials present, these samples are well-known analogues to Martian regolith. All samples were GPS-coded, cached on site, placed in sealed vials, and maintained in a sterile desiccator until used. Details related to the collection sites for the samples used in this manuscript are included in Table 1. For sample preparation using our proposed platform, an aliquot of 10 mg of soil was added to 10 mL of running buffer and stirred in an ultrasonic bath for 10 min. One mL of this was centrifuged at 13 400 rpm for 15 min and the supernatant was injected hydrodynamically in the electrophoretic system. Additional information related to these samples, the collection sites, and corresponding μchip-CE analysis for organic species can be found elsewhere.[35]

In order to verify the results obtained with the proposed platform, the elemental composition of the soil samples was analyzed by energy dispersive X-ray spectroscopy (EDX). The experiments were performed by placing an aliquot of the sample in a Hitachi High Resolution 5500 SEM Scanning electron microscope, equipped with an XFlash 4010 Si drift detector (Bruker AXS; Billerica, MA) and operated at 30 kV. The data, collected over an approximate area of 50 μm^2, was analyzed with built-in software (Quantax Espirit 1.9).

Safety considerations

The high voltage power supply and associated open electrical connections should be handled with extreme care to prevent electrical shock.

3 Results and discussion

Although we foresee a wide number of potential applications, the goal of this manuscript was to demonstrate the characteristics and advantages of the proposed platform through the analysis of inorganic cations in soil samples. Key factors affecting the performance of the platform were investigated and are discussed.

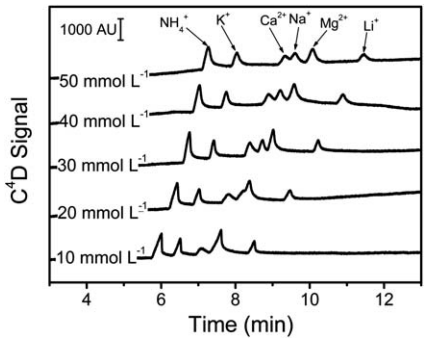

Fig. 2 Effect of the concentration of equimolar MES and HIS buffer (pH = 6.1) on the separation of the selected cations, at 100 μmol L^{-1} each. *Other conditions*: 3 mmol L^{-1} 18-crown-6, E_{SEP} = 10 kV, capillary length = 60 cm, effective length = 56 cm, 5 s hydrodynamic injection.

Effect of buffer solution

Similar to conventional CE, the buffer solution has a significant effect on the analysis because it influences the total charge of analytes, the magnitude of the EOF, and the generation of Joule heating (which could affect resolution). Furthermore, as previously reported, the buffer system also has a considerable effect on the signal/noise obtained in C^{4}D.[36,37] Therefore, an equimolar MES and HIS buffer, pH = 6.1 + 2 mmol L^{-1} 18-crown-6 was selected based on previous literature reports.[38–40] Although this background electrolyte was selected as a simple solution to demonstrate the functionality of the system, alternative conditions[41,42] could be selected to provide improved the resolution, if needed.

The effect of the buffer concentration on the separation and detection was evaluated in the 10–50 mmol L^{-1} range (for each component) by injecting a standard solution containing 100 μmol L^{-1} of the six cations diluted in the same buffer. As observed in Fig. 2, concentrations ≥30 mmol L^{-1} MES and 30 mmol L^{-1} HIS yielded significant increases in the overall analysis time but enabled the identification of all six selected cations. This behavior can be attributed to a decrease in the effective charge of the surface of the capillary, shielded by the increasing concentration of ions in the background electrolyte. It is also important to note that, within the investigated range of buffer concentrations, the signal/noise was not adversely affected. Considering these results, and as a balance between resolution and analysis time, 30 mmol L^{-1} MES and 30 mmol L^{-1} HIS pH = 6.1 (+3 mmol L^{-1} 18-crown-6, *vide infra*) was selected as the optimum background electrolyte and used for the rest of experiments described in this manuscript.

Table 1 Information related to the mineralogy and location sites of soil samples collected from the Atacama Desert

Label	Mineralogy	Depth	Latitude	Longitude	Elevation
AT40B1-08	Exposed duracrust	<1 cm	S24°03.629′	W69°52.092′	1081 m
AT44B1-08	Exposed duracrust	<1 cm	S24°03.651′	W69°52.102′	1075 m
AT54A1-08	Duracrust	2–3 cm	S24°03.680′	W69°52.098′	1055 m

Effect of buffer additives

It is well-known that the separation of some cations can be optimized by the addition of 18-crown-6 to the running electrolyte.[43] The main reason for this is that 18-crown-6 is able to form inclusion complexes with several inorganic cations, which affects the effective electrophoretic mobility of the cations and imparts selectivity to the separation step.[44] Consequently, the effect of the concentration of 18-crown-6 on the separation was investigated in the 0–5 mmol L^{-1} range, using 30 mmol L^{-1} MES and 30 mmol L^{-1} HIS buffer as the running electrolyte. The results are summarized in Fig. 3. In line with previous reports, where the stability complex constant of K^+ with 18-crown-6 (log $K_s = 2.1$) was reported to be significantly higher than that of NH_4^+ (log $K_s = 1.01$),[43] sequential additions of 18-crown-6 only influenced the migration time of the peak corresponding to potassium, enabling its separation from NH_4^+ with as little as 1 mmol L^{-1}. In order to maximize the separation and minimize the possibility of co-migration with other species present in the target samples, a concentration of 3.0 mmol L^{-1} 18-crown-6 was selected and used for all the experiments described in this manuscript.

It is also important to highlight that Tanyanyiwa and Hauser[38] stated that although it is possible to achieve complete resolution of the ammonium and potassium peaks using long capillaries and concentrations of 18-crown-6 as low as 1 mmol L^{-1}, it would not be possible to resolve them on glass chips with less than 2 mmol L^{-1}. In such cases,[45] concentrations as high as 7.5 mmol L^{-1} would be required. The results shown in Fig. 3 (where baseline separation of the ammonium and potassium peaks was achieved) strongly indicate that the proposed platform is able to offer not only the advantages of most microfluidic systems but also a performance that is comparable to standard bench-top instruments.

Effect of capillary length

Generally, increasing the effective length of the capillary is beneficial to separation efficiency and resolution of separations under diffusion-limited conditions.[46,47] Although replacing the capillary in most commercial bench-top systems is not complicated, the operation must be manually performed

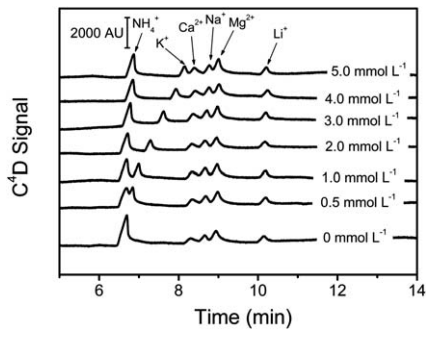

Fig. 3 Effect of the concentration of 18-crown-6 on the separation of the selected cations at 100 μmol L^{-1} each. *Conditions*: 30 mmol L^{-1} MES and 30 mmol L^{-1} HIS, E_{SEP} = 10 kV, capillary length = 60 cm, effective length = 56 cm, 5 s hydrodynamic injection.

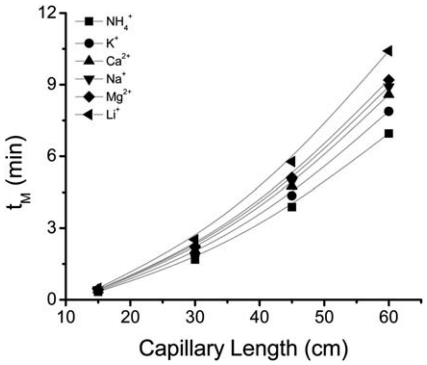

Fig. 4 Effect of the capillary length on the separation of the selected cations at 100 μmol L^{-1} each. *Conditions*: E_{SEP} = 10 kV, 30 mmol L^{-1} MES and 30 mmol L^{-1} HIS + 3 mmol L^{-1} 18-crown-6 as running buffer; 5 s hydrodynamic injection. Original electropherograms included as ESI.†

(reassembling the capillary cartridge) and is often limited to fixed increments.[47] At the microchip-scale, changing the length of the separation channel is significantly more challenging. For that reason, most designs include separation channels in the range of a few centimeters or require the implementation of serpentine geometries which can induce dispersion.[48] Therefore, in order to demonstrate the possibility to change and customize the capillary length in the proposed design, the effect of four different capillary lengths on the separation was investigated: 15 cm, 30 cm, 45 cm and 60 cm (effective lengths of 11 cm, 26 cm, 41 cm, and 56 cm, respectively). As observed in Fig. 4, significant increases in the analysis times and separation efficiencies were obtained when the separation was performed using longer capillaries. In the case of the 60 cm-long capillary (using the conditions described in Fig. 4), an average of 17 000 plates per m was obtained (ranging from 7 300 plates per m for NH_4^+ to 27 000 plates per m for Na^+). The resolution, calculated for the 60 cm capillary and the conditions described in Fig. 4, ranged from 1.1 (for the peaks corresponding to Ca^{2+} and Na^+) to 3.4 (for the peaks corresponding to Mg^{2+} and Li^+). Based on these results, 60 cm was selected as the optimum length and was used for all the subsequent experiments described in this manuscript.

Effect of injection time

At any scale, obtaining a reproducible and representative sample injection has been deemed paramount for quantitative analytical applications.[49] Although injections in microchips routinely rely on some variant of electrokinetic injection[2,50] (due to its simplicity), its performance can be significantly affected by EOF velocity, sample bias, sample conductivity, and electrolysis effects. Since these issues are particularly important for the analysis of small ions with high electrophoretic mobility, hydrodynamic injection (applying vacuum on the sample waste reservoir, for example) was selected for the experiments described in this manuscript. Besides being reproducible, this method avoids the use of additional hardware and is significantly simpler than previously proposed sample injection methods.[51,52] Although preliminary experiments were performed using a soldering iron pump (1700, Paladin Tools, USA),

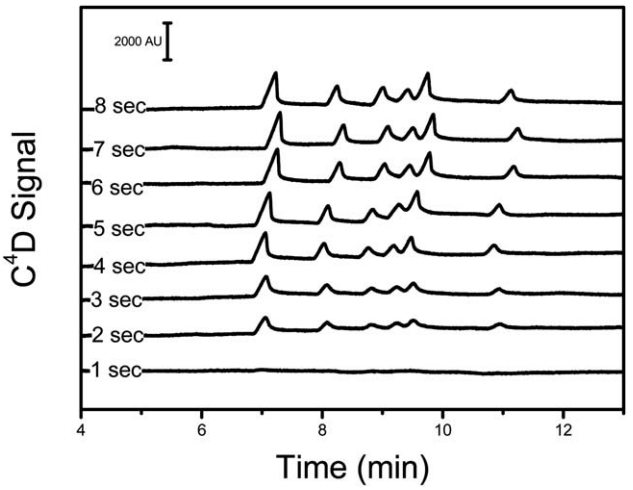

Fig. 5 Effect of the injection time on the signal magnitude. Hydrodynamic injections were performed applying vacuum (~70 kPa) on the SW reservoir for the selected times. Migration order is as shown in previous figures.

the house vacuum line (~70 kPa) was used for the experiments herein described. The selected method yielded comparable results while enabling the control of the injection time. Next, the effect of injection time on signal magnitude was investigated over a range of 1–8 s. As it can be observed in Fig. 5, significant increases in signal (proportional to the injection time) were obtained in the 1–6 s range. As further increases in injection time (in the 6–8 s range) did not yield improvements in signal/noise, 6 s was adopted as the optimal time for injection. Notably, no significant peak distortion was observed within the selected times, suggesting that only the center of the interconnect is being filled and that the sample plug is being pinched with flow from the separation channel and buffer reservoir.

Analytical figures of merit

Using the optimized conditions for the separation and detection (10 kV as the separation potential, 30 mmol L^{-1} MES and 30 mmol L^{-1} HIS pH = 6.1 + 2 mmol L^{-1} 18-crown-6 as running buffer; 6 s hydrodynamic injection, and 60 cm capillary), linear relationships between the concentration and the C^4D signal were obtained for the six cations analyzed up to 500 μM. At higher concentrations, significant co-migration of the ions was observed, precluding the analysis. The limit of detection for each cation was estimated using a signal/noise ratio of at least 3, obtained upon the injection of samples under the optimum conditions. The results corresponding to each calibration curve are summarized in Table 2.

The proposed system provided similar sensitivity to other microfluidic systems coupled to C^4D[53] and conventional capillary electrophoresis systems when coupled to either indirect UV-Vis[54] or conductivity detection.[55] Although these values were considered appropriate for the target application, alternative configurations can be selected to further improve the sensitivity.[56]

Table 2 Migration time (t_M), sensitivity, coefficient of determination (R^2), and calculated limit of detection (LOD) corresponding to the analysis of the selected inorganic cations under optimal conditions

Cation	t_M (min)	Sensitivity (AU μmol^{-1} L)	R^2	LOD (μmol L^{-1})
NH_4^+	7.1 ± 0.1	7.7 ± 0.2	0.99	7
K^+	8.2 ± 0.1	4.1 ± 0.1	0.99	53
Ca^{2+}	8.9 ± 0.1	4.1 ± 0.1	0.99	38
Na^+	9.3 ± 0.1	4.9 ± 0.2	0.99	57
Mg^{2+}	9.6 ± 0.1	9.9 ± 0.5	0.98	45
Li^+	11.0 ± 0.1	3.2 ± 0.2	0.98	91

Analysis of soil samples

The identification and quantification of the components of each sample were performed by comparing the electropherograms obtained with standard solutions to those obtained with the corresponding samples under the optimal conditions. A main peak at 8.9 min was observed in all samples (data available in the ESI†), with a migration time matching that of Ca^{2+}. In two samples (AT40B1-44 and AT40B1-54), it was also possible to identify a second peak with much lower intensity that was assigned to Na^+. Based on the peak intensity, the amount of Ca^{2+} was 20.4, 44.1, and 78.2 mg of Ca^{2+} per gram of soil in the samples marked as ATB1-40, ATB1-44, and ATB1-54, respectively. These findings are in agreement not only with previous reports describing the abundance of $CaSO_4$ in such samples, but also with the results obtained by EDX (see ESI†).

4 Conclusions

A new hybrid device, based on the use of 5 plastic microfluidic components, was fabricated quickly and inexpensively. Additionally, the new platform bypasses some of the traditional problems involving microchip fabrication, including large/specific machineries and lengthy assembly times. The platform itself is highly versatile and can be coupled with a number of inline detection methods, such as C^4D or UV-Vis. The variable length of the separation channel adds another advantage in that the separations can be adjusted if necessary. The simplicity of the platform allows for customization in terms detection, capillary length, injection type (gated and pinched electrokinetic or hydrodynamic), and reservoir volumes. This device is an attractive approach for portable analytical instrumentation capable of performing rapid analyses, as demonstrated through the conductometric detection of inorganic cations.

Acknowledgements

The authors gratefully acknowledge the financial support provided by STTN/NASA (NNX12CG20P-1), The University of Texas at San Antonio and the National Institutes of Health through the National Institute of General Medical Sciences (1SC3GM081085, 2SC3GM081085), the NASA Astrobiology Science and Technology Development (ASTID) Program (104320), and the Research Centers at Minority Institutions (G12MD007591).

References

1 G. V. Kaigala, V. N. Hoang, A. Stickel, J. Lauzon, D. Manage, L. M. Pilarski and C. J. Backhouse, *Analyst*, 2008, **133**, 331–338.
2 D. Wu, J. Qin and B. Lin, *J. Chromatogr., A*, 2008, **1184**, 542–559.
3 X. Liu, R. C. Lo and F. A. Gomez, *Electrophoresis*, 2009, **30**, 2129–2133.
4 J. P. Kutter, *J. Chromatogr., A*, 2012, **1221**, 72–82.
5 E. T. da Costa, C. A. Neves, G. M. Hotta, D. T. Vidal, M. F. Barros, A. A. Ayon, C. D. Garcia and C. L. do Lago, *Electrophoresis*, 2012, **33**, 2650–2659.
6 M. F. Mora, F. Greer, A. M. Stockton, S. Bryant and P. A. Willis, *Anal. Chem.*, 2011, **83**, 8636–8641.
7 I. Rodriguez, Y. Zhang, H. K. Lee and S. F. Li, *J. Chromatogr., A*, 1997, **781**, 287–293.
8 D. Solignac, A. Sayah, S. Constantin, R. Freitag and M. A. M. Gijs, *Sens. Actuators, A*, 2001, **A92**, 388–393.
9 A. Berthold, F. Laugere, H. Schellevis, C. R. de Boer, M. Laros, R. M. Guijt, P. M. Sarro and M. J. Vellekoop, *Electrophoresis*, 2002, **23**, 3511–3519.
10 H. Becker and L. Locascio, *Talanta*, 2002, **56**, 267–287.
11 M. Castano-Alvarez, M. T. Fernandez-Abedul and A. Costa-García, *Electrophoresis*, 2005, **26**, 3160–3168.
12 B. Graß, A. Neyer, M. Johnck, D. Siepe, F. Eisenbeiß, G. Weber and R. Hergenroder, *Sens. Actuators, B*, 2001, **72**, 249–258.
13 Y. Liu, D. Ganser, A. Schneider, R. Liu, P. Grodzinski and N. Kroutchinina, *Anal. Chem.*, 2001, **73**, 4196–4201.
14 D. C. Duffy, J. C. McDonald, O. J. A. Schueller and G. M. Whitesides, *Anal. Chem.*, 1998, **70**, 4974–4984.
15 J. C. McDonald and G. M. Whitesides, *Acc. Chem. Res.*, 2002, **35**, 491–499.
16 M. A. Roberts, J. S. Rossier, P. Bercier and H. Girault, *Anal. Chem.*, 1997, **69**, 2035–2042.
17 G. B. Lee, S. H. Chen, G. R. Huang, W. C. Sung and Y. H. Lin, *Sens. Actuators, B*, 2001, **B75**, 142–148.
18 H. Shadpour, H. Musyimi, J. Chen and S. A. Soper, *J. Chromatogr., A*, 2006, **1111**, 238–251.
19 M. Rahbar, S. Chhina, D. Sameoto and M. Parameswaran, *J. Micromech. Microeng.*, 2010, **20**, 015026.
20 F. Abbasi, H. Mirzadeh and A.-A. Katbab, *Polym. Int.*, 2001, **50**, 1279–1287.
21 D. Belder and M. Ludwig, *Electrophoresis*, 2003, **24**, 3595–3606.
22 C. D. Garcia, B. M. Dressen, A. Henderson and C. S. Henry, *Electrophoresis*, 2005, **26**, 703–709.
23 S. Hu, X. Ren, M. Bachman, C. E. Sims, G. P. Li and N. Allbritton, *Anal. Chem.*, 2002, **74**, 4117–4123.
24 Y. Wang and P. L. Dubin, *Anal. Chem.*, 1999, **71**, 3463–3468.
25 A. Muck and A. Svatoš, *Talanta*, 2007, **74**, 333–341.
26 E. F. M. Gabriel, G. F. Duarte Junior, P. d. T. Garcia, D. P. de Jesus and W. K. T. Coltro, *Electrophoresis*, 2012, **33**, 2660–2667.
27 A. W. Martinez, S. T. Phillips, M. J. Butte and G. M. Whitesides, *Angew. Chem., Int. Ed.*, 2007, **46**, 1318–1320.
28 A. W. Martinez, S. T. Phillips and G. M. Whitesides, *Proc. Natl. Acad. Sci. U. S. A.*, 2008, **105**, 19606–19611.
29 A. W. Martinez, S. T. Phillips, G. M. Whitesides and E. Carrilho, *Anal. Chem.*, 2009, **82**, 3–10.
30 P. K. Yuen, *Lab Chip*, 2008, **8**, 1374–1378.
31 M. Rhee and M. A. Burns, *Lab Chip*, 2008, **8**, 1365–1373.
32 S. M. Langelier, E. Livak-Dahl, A. J. Manzo, B. N. Johnson, N. G. Walter and M. A. Burns, *Lab Chip*, 2011, **11**, 1679–1687.
33 A. Chen and T. Pan, *Lab Chip*, 2011, **11**, 727–732.
34 K. J. M. Francisco and C. L. do Lago, *Electrophoresis*, 2009, **30**, 3458–3464.
35 A. M. Skelley, A. D. Aubrey, P. A. Willis, X. Amashukeli, P. Ehrenfreund, J. L. Bada, F. J. Grunthaner and R. A. Mathies, *J. Geophys. Res.*, 2007, **112**, G04S11.
36 J. G. A. Brito-Neto, J. A. Fracassi da Silva, L. Blanes and C. L. do Lago, *Electroanalysis*, 2005, **17**, 1207–1214.
37 J. G. A. Brito-Neto, J. A. Fracassi da Silva, L. Blanes and C. L. do Lago, *Electroanalysis*, 2005, **17**, 1198–1206.
38 J. Tanyanyiwa and P. C. Hauser, *Anal. Chem.*, 2002, **74**, 6378–6382.
39 K. A. Mahabadi, I. Rodriguez, C. Y. Lim, D. K. Maurya, P. C. Hauser and N. F. de Rooij, *Electrophoresis*, 2010, **31**, 1063–1070.
40 M. Pumera, J. Wang, F. Opekar, I. Jelínek, J. Feldman, H. Löwe and S. Hardt, *Anal. Chem.*, 2002, **74**, 1968–1971.
41 M. Mori, M. Kaseda, T. Yamamoto, S. Yamada and H. Itabashi, *Anal. Bioanal. Chem.*, 2012, **402**, 2425–2430.
42 S. D. Noblitt and C. S. Henry, in *Capillary Electrophoresis and Microchip Capillary Electrophoresis. Principles, Applications, and Limitations*, ed. C. D. Garcia, K. Chumbimuni-Torres and E. Carrilho, John Wiley & Sons, Hoboken, NJ, 2013, pp. 177–200.
43 C. Francois, P. Morin and M. Dreux, *J. Chromatogr., A*, 1995, **706**, 535–553.
44 P. Kubáň, P. Kubáň and V. Kubáň, *Electrophoresis*, 2002, **23**, 3725–3734.
45 J. Wang, M. Pumera, G. Collins, F. Opekar and I. Jelinek, *Analyst*, 2002, **127**, 719–723.
46 A. E. Karger, *Electrophoresis*, 1996, **17**, 144–151.
47 S. Oguri, M. Hibino and M. Mizunuma, *Electrophoresis*, 2004, **25**, 1810–1816.
48 V. Dolnik, S. Liu and S. Jovanovich, *Electrophoresis*, 2000, **21**, 41–54.
49 R. M. Saito, W. K. T. Coltro and D. P. de Jesus, *Electrophoresis*, 2012, **33**, 2614–2623.
50 M. Gong, K. R. Wehmeyer, A. M. Stalcup, P. A. Limbach and W. R. Heineman, *Electrophoresis*, 2007, **28**, 1564–1571.
51 J. Wang, G. Chen, A. Muck, Jr and G. E. Collins, *Electrophoresis*, 2003, **24**, 3728–3734.
52 L. Zhang, X. Yin and Z. Fang, *Lab Chip*, 2006, **6**, 258–264.
53 T. P. Segato, W. K. T. Coltro, A. L. de Jesus Almeida, M. H. de Oliveira Piazetta, A. L. Gobbi, L. H. Mazo and E. Carrilho, *Electrophoresis*, 2010, **31**, 2526–2533.
54 W. Beck and H. Engelhardt, *Chromatographia*, 1992, **33**, 313–316.
55 J. A. Fracassi da Silva and C. L. do Lago, *Anal. Chem.*, 1998, **70**, 4339–4343.
56 J. Tanyanyiwa, B. Galliker, M. A. Schwarz and P. C. Hauser, *Analyst*, 2002, **127**, 214–218.